

## SYNTHETIC DIAGRAMS FOR THE INTERPRETATION OF SFR AND IMF IN THE PRELIMINARY HIPPARCOS H30 HR DIAGRAM

G. Bertelli<sup>1,2</sup>, E. Nasi<sup>3</sup>, A. Bressan<sup>3</sup>, C. Chiosi<sup>1</sup>

<sup>1</sup>Astronomy Department, Vicolo dell'Osservatorio 5, 35122 Padova, Italy

<sup>2</sup>National Council of Research (CNR-GNA), Rome, Italy

<sup>3</sup>Astronomical Observatory, Vicolo dell'Osservatorio 5, 35122 Padova, Italy

### ABSTRACT

Stellar populations of the solar neighbourhood can be investigated with the method of the synthetic HR diagrams based on suitable assumptions for the star formation rate, the initial mass function, and the metallicity. The analysis of the HR diagram based on the Hipparcos H30 catalogue (Perryman et al. 1995) allows to infer preliminary indications on metal content, IMF and past history of star formation of the underlying stellar population. This method will show its full capability when the space distribution of stars in the sample and the observational uncertainties will be taken into account after the release of the Hipparcos data.

Key words: space astrometry; HR diagram; stellar content.

### 1. INTRODUCTION

Perryman et al. (1995) presented preliminary considerations on the statistical properties of the Hipparcos H30 catalogue and described the main features of the observational Hertzsprung-Russell diagram. Their Figure 6a displays 8784 stars, whose relative parallax error is less than 0.1 and whose photoelectric standard error for  $(B - V)$  is less than 0.025 mag. Photometric data involved in the discussion of Hipparcos data are: (a) broad band Hp magnitudes derived from the Hipparcos main instrument; (b) V magnitudes and  $B - V$  colour indices derived from ground-based photometry. The Hipparcos magnitude, Hp, is defined by the pass-band of the Hipparcos main detection chain, which ranges from 340 to 850 nm (Grenon et al. 1992, Turon et al. 1992, Perryman et al. 1995). The interpretation of this HR diagram in terms of local stellar population requires evaluations of the chemical composition, age, initial mass function (IMF), and star formation rate (SFR) of the solar neighbourhood. With the aid of synthetic HR diagrams, based on a homogeneous set of stellar models for the adopted range of chemical composition and various choices for the IMF and the SFR, we attempted to constrain the related parameters in

such a way as to give a reasonable interpretation of the main features of the Perryman et al. HR diagram and to evaluate the star formation history of the galactic disc.

Taking into account the observability limit of the satellite (Perryman et al. 1995), we adopted 4.5 mag as a reasonable value of the absolute magnitude  $M_{Hp}$  at which the sample can be considered complete (for all observed stars within 50 pc of the Sun). This means that in our analysis we considered the sample as containing all stars of the solar neighbourhood more luminous than  $M_{Hp} = 4.5$  mag and evaluated the distribution of stars in the synthetic diagrams with this limiting magnitude.

### 2. SYNTHETIC HR DIAGRAMS

The fundamental ingredient of this analysis is the computation of synthetic HR diagrams. To simulate the colour-magnitude diagram of stars observed with Hipparcos in the solar neighbourhood, stars were randomly placed in the synthetic HR-diagram according to an assumed star formation rate (SFR), initial mass function (IMF) and suitable range of metallicity. Stellar evolutionary models by Bressan et al. (1993) and Fagotto et al. (1994a, 1994b) are used. These models extend over all the evolutionary phases from the zero age main sequence to the start of the thermally pulsing AGB or carbon-ignition as appropriate to the initial mass of the stars.

For the star formation rate the assumptions used in the models will be explained in Section 3 with all the required details. For the IMF the classical Salpeter law is used in the form:

$$dN \propto M^{-x} dM$$

where  $x$  is a free parameter to be fixed by imposing observational constraints suggested from the comparison with Hipparcos observations. We have analyzed two possibilities for the  $x$  value:  $x = 2.35$  (the Salpeter case) and  $x = 0.35$ , a very flat IMF, so that to evidentiate in the diagrams the effects of a rather different slope of the IMF.

For temperatures hotter than 4000 K we used Kurucz' atmosphere models (1992) for the determina-

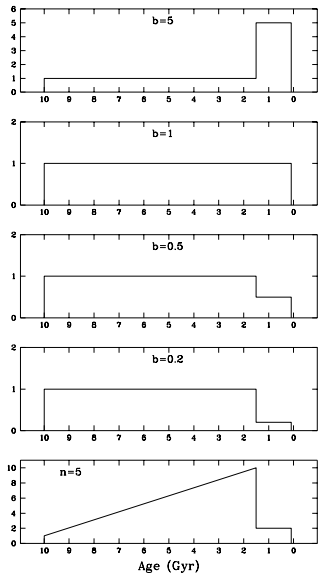


Figure 1. The schematic shape of the SFR in the two time intervals (from 10 to 1.5 Gyr and from 1.5 to 0.1 Gyr) is shown as used in the simulations, considering four cases for the ratio of the rate in the second interval over that in the first one, described by the parameter  $b$ . In the fifth case the SFR is increasing up to the value at 1.5 Gyr and then it is reduced to  $1/5$  of the previous final value.

tion of magnitudes and colors in the useful passbands, as in Bertelli et al. (1994). At lower temperatures, waiting for improved model photospheres of M dwarfs, in order to convert the effective temperature from theoretical models into the  $(B - V)$  color index, we adopted the temperature scale for cool dwarfs by Bessell (1995), linking it to the  $(B - V)$  color-index (Bessell 1991) through  $(V - I)$  and  $M_I$  values.

### 3. COMPARISON WITH H30 CMD

It is worth clarifying from the very beginning that the discussion below is entirely based on the comparison between the morphological appearance of the synthetic HR diagrams and the observed one. No use of the luminosity function star counts is yet possible. In order to explain the main features of the observed HR diagram, we superimpose on it a few selected isochrones with solar chemical composition, and evidence the following points:

- (i) the star formation began about 10 Gyr ago and stopped around 100 million years ago;
- (ii) there is a sudden change in the apparent main sequence star density around  $M_{Hp} = 2.5$ , which can be interpreted as a discontinuity in the SFR in correspondence to an age of about 1.5 Gyr ( $t_{\text{sep}}$ );
- (iii) stars beyond main sequence and less luminous than the horizontal branch are characterized by a widespread and almost uniform distribution.

(iv) the HB clump is too broadened to be explained by the presence of mere solar chemical composition.

It is evident from the width of the main sequence band and also from the color extension of the horizontal branch clump that there is an extended range of chemical composition of the observed stars. From the comparison between isochrones with different metal content (Bertelli et al. 1994) and observations we evaluate that the majority of the stars must have a chemical composition in the range  $0.008 \leq Z \leq 0.03$ . This choice of the chemical composition is supported also by the results of extensive spectroscopic observations of selected nearby F and G stars from the paper by Edvarsson et al. (1993) on the chemical evolution of the galactic disk. Taking into account observations and models, we compute synthetic HR diagrams supposing that stars have a metallicity  $Z$  randomly chosen between 0.008 and 0.03.

All simulations are done by requiring a fixed number of stars in the horizontal branch clump. After a series of simulations we evaluated that a number of 300 HB stars could give solutions in satisfactory agreement with observations (i.e. with the total number of stars and with the relative distribution in different regions of the Hipparcos HR diagram).

The whole time range considered in the simulations has been splitted in two intervals: the first one  $\Delta t_1$  from 10 Gyr to  $t_{\text{sep}}$  and the second one  $\Delta t_2$  from  $t_{\text{sep}}$  to  $10^8$  years ago.

Different hypotheses are investigated for the star formation rate, using the simplest case of a two phases model. In the first four cases of Figure 1 there is a discontinuity at the age  $t_{\text{sep}}$  and there is only one parameter characterizing each case: the ratio  $\mathbf{b}$  of the SFR in the interval  $\Delta t_2$  over the value in the interval  $\Delta t_1$  ( $\mathbf{b}$  varies in the range between 5 and 0.2). The fifth case of Figure 1 considers a growing rate in the first interval  $\Delta t_1$ , with a final value ten times the initial one, and a constant rate (in the second interval  $\Delta t_2$ ) equal to  $1/5$  of the previous final value. This example is shown to evaluate the sensibility of the method to formulations of the SFR different from the simple ones analysed previously.

Figures 2a and 2b show the first case of star formation history which corresponds to a recent star formation rate more efficient than in the past ( $\mathbf{b} = 5$ ), with  $x = 0.35$  and  $x = 2.35$ , respectively, for the IMF.

Figures 3a and 3b show the third case with a recent SFR less efficient than in the past ( $\mathbf{b} = 0.5$ ). Not all the considered cases are shown for the sake of simplicity, but the comparison of the different synthetic diagrams with Hipparcos H30 HR diagram allows us to make the following considerations.

The simulations taking into account a recent SFR more efficient than in the past (case  $\mathbf{b} > 1$ ) could account for the apparent distribution of evolved stars, if  $\mathbf{b}$  is suitably chosen together with a steep slope for the IMF ( $x = 2.35$ ). However they cannot reproduce the density discontinuity of stars along the MS.

Adopting a recent SFR less efficient than in the past (cases  $\mathbf{b} < 1$ ) with a convenient choice of the parameter  $\mathbf{b}$  together with a low value of the IMF parameter ( $x = 0.35$ ), all the characteristic features of the

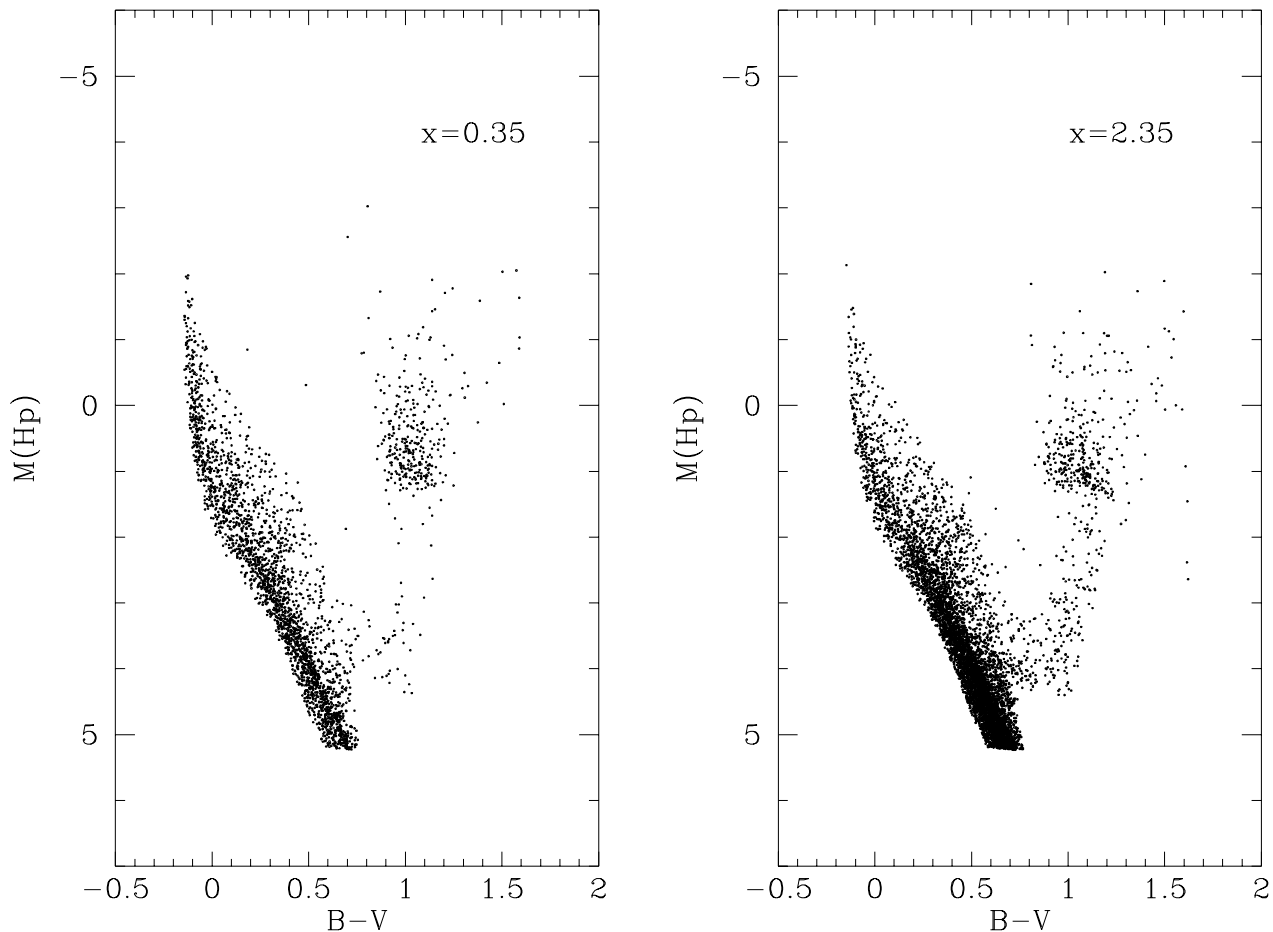


Figure 2. Synthetic HR diagrams computed for the first case correspondent to a recent star formation rate more efficient than in the past ( $b = 5$ ). For the initial mass function in panel (a) the value  $x=0.35$  is adopted and in panel (b)  $x=2.35$ .

observed HR diagram can be reproduced. In particular Figure 3a which displays the third case of SFR ( $\mathbf{b} = 0.5$ ), looks fairly similar to the upper part of Figure 6a by Perryman et al. (1995).

The HR diagram derived for the fifth case of the SFR is shown in Figures 4a and 4b. Also in this case we can consider very good the agreement between the simulation (Figure 4a, case  $x = 0.35$ ) and the observed diagram, as the distribution of evolved stars is fairly homogeneous. This is due to the increasing SFR (in the first time interval  $\Delta t_1$ ), which enhances the more massive stars number, in addition to the same effect produced also by the low value of the IMF slope.

In summary the comparison of the synthetic HR diagrams with the observed distribution seems to favour a solution characterized by:

- IMF slope flatter than Salpeter (we tested the value  $x = 0.35$  to make more evident the differences);
- constant or increasing SFR from about 10 to 1.5 Gyr ago;

- thereafter reduced value of the SFR ( $\mathbf{b} = 1/2, 1/3$ ) compared to the maximum value of the previous phase.

However we remind that the apparent discontinuity in the density distribution of stars along the main sequence might simply be an optical effect, due to different number of stars producing different darkening. This feature will be explicitly evaluated when the observed number distributions are available.

#### 4. CONCLUSIONS

The previous comparison of the observed HR diagram with the synthetic ones suggests the following considerations:

- There is a large spread in metallicity, confirmed by our analysis with the synthetic diagrams, being unable to reproduce the observed star distribution with a fixed chemical composition. Edvardsson et al. (1993) in their paper on the chemical evolution of the galactic disk concluded that there is not a well

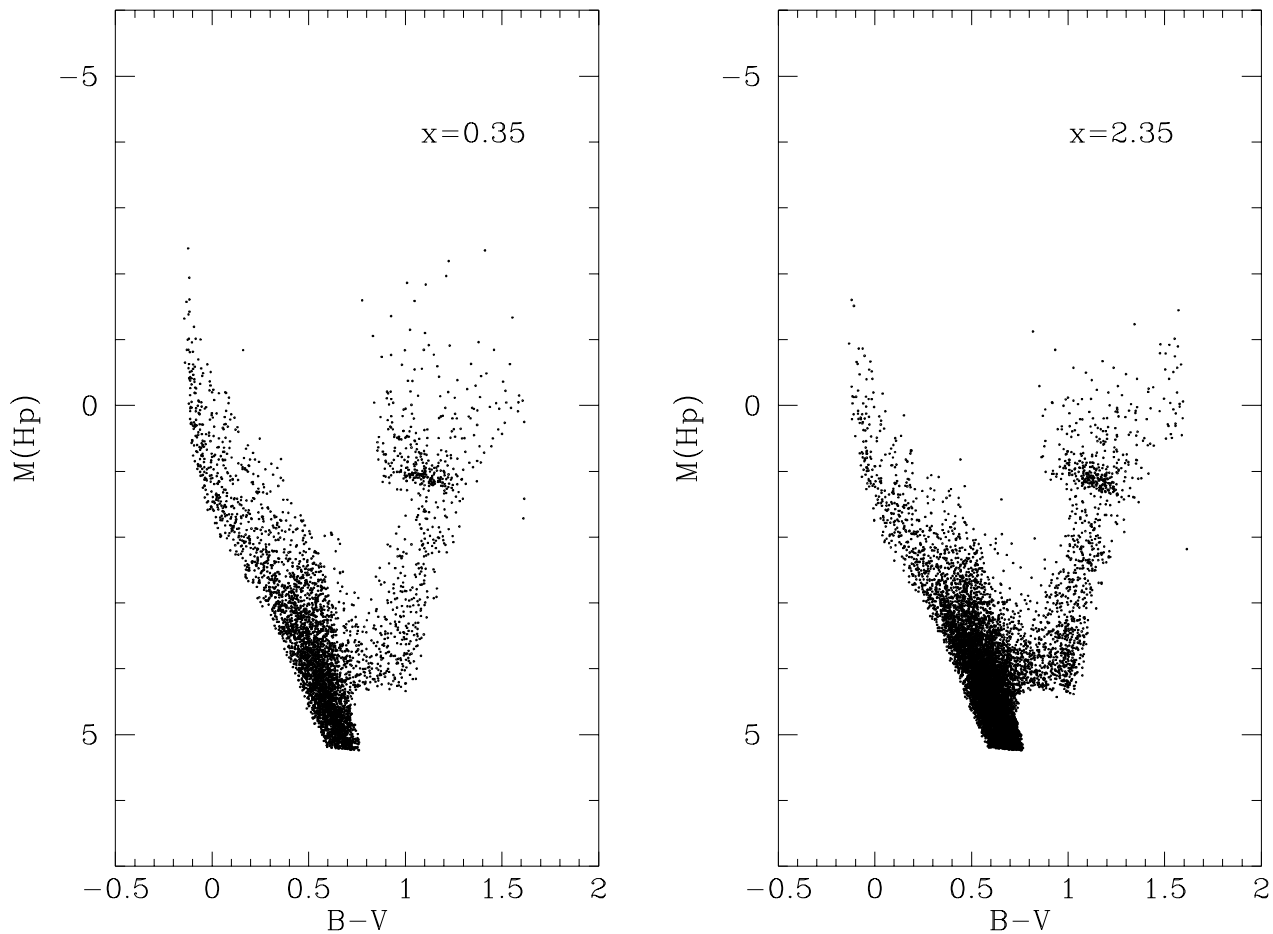


Figure 3. Synthetic HR diagrams computed for the third case correspondent to a recent star formation rate less efficient than in the past ( $b = 0.5$ ). For the initial mass function in panel (a) the value  $x=0.35$  is adopted and in panel (b)  $x=2.35$ .

defined age-metallicity relation and it looks like as the average metallicity of the disk has increased by very little over the disk's lifetime with the scatter at all times almost as large as the difference between the average metallicity then and now, for stars born at roughly the same galactocentric distance.

Moreover if the feature described at point (ii) of Section 2 is real, also the following two indications must be considered:

- The star distributions along the main sequence and in the subgiant region are better described by an IMF flatter than the Salpeter one;
- The star formation rate in the past (from about 10 to 1.5 Gyr ago) must have been higher than more recently (from 1.5 to 0.1 Gyr ago). The rate might have been constant or increasing in the first interval, and significantly lower (of a factor 2–5) during the last 1.5 Gyr. Such a preliminary conclusion is at odds with the results by Chiappini et al. (1997), obtained studying the chemical properties of the solar vicinity with a two-infall model. In fact they suggest a SFR overall decreasing during the last 10 Gyrs, but there

is agreement in the evaluation of a low star formation rate since 1.5 Gyr ago.

When the observational data will be available we will be able to determine quantitatively the IMF and the SFR adopting a technique already successfully experimented in the study of the fields in LMC (Bertelli et al. 1992, Vallenari et al. 1996a, 1996b) and in the analysis of the stellar content and SFR of dwarf galaxies (Gallart et al. 1994, 1996). The analysis will be performed taking into account the observational uncertainties, the spatial distribution of observed stars and the completeness of the sample.

#### ACKNOWLEDGMENTS

This study has been financially supported by the Italian Ministry of University, Scientific Research and Technology (MURST) and the Italian Space Agency (ASI).

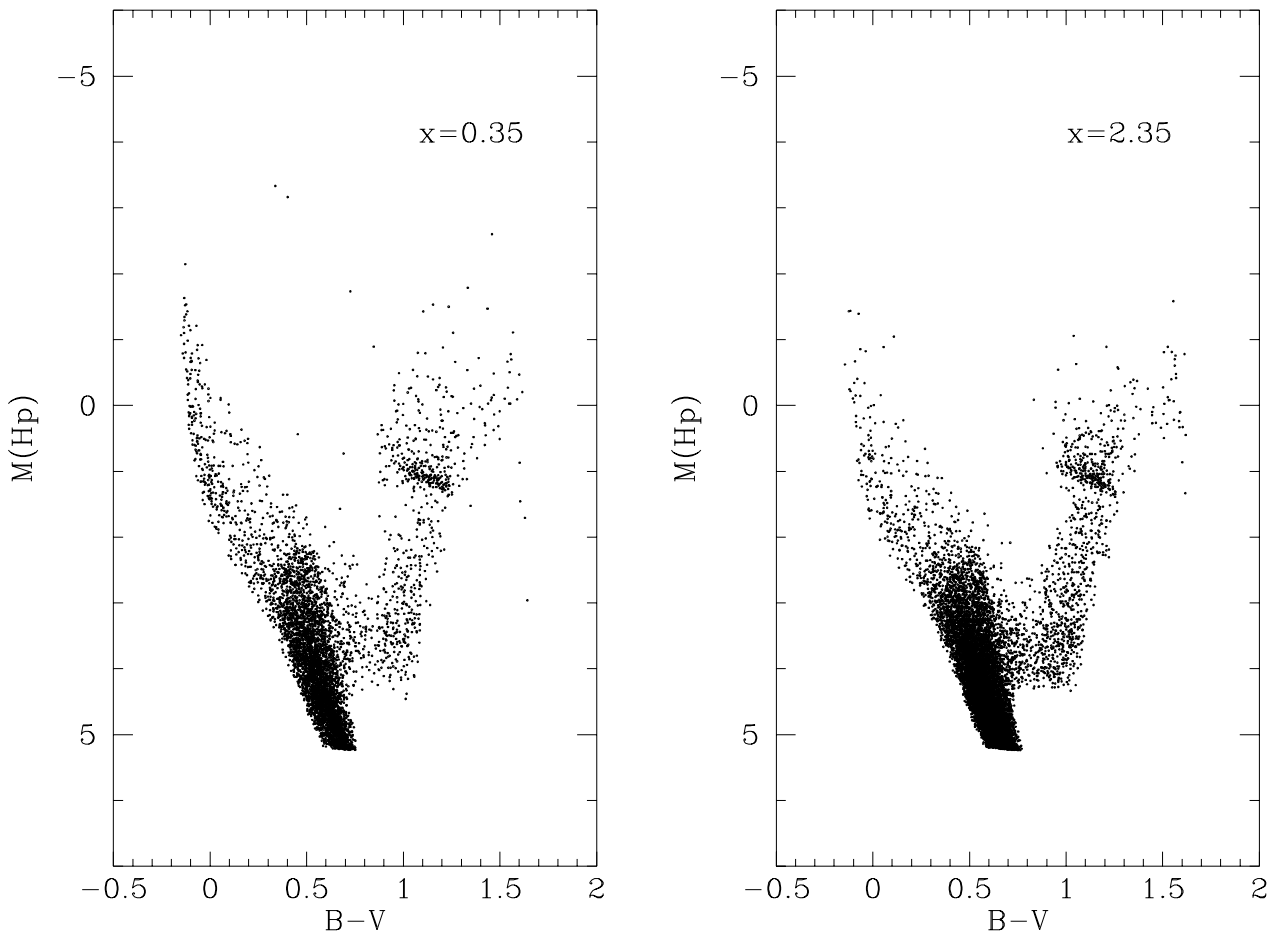


Figure 4. Synthetic HR diagrams computed for the fifth case correspondent to a star formation rate increasing in the first time interval and a recent SFR less efficient than in the past ( $1/5$  of the previous final value). For the initial mass function in panel (a) the value  $x=0.35$  is adopted and in panel (b)  $x=2.35$ .

#### REFERENCES

- Bertelli, G., Mateo, M., Chiosi, C., Bressan, A., 1992, *ApJ*, 388, 400
- Bertelli, G., Bressan, A., Chiosi, C., Fagotto, F., Nasi, E., 1994, *A&AS*, 106, 275
- Bessell, M.S., 1991, *AJ*, 101, 662
- Bessell, M.S., 1995, in 'The Bottom of the Main Sequence and Beyond', ESO Symp., ed. C.G. Tinney, p.123
- Bressan, A., Fagotto, F., Bertelli, G., Chiosi, C. 1993, *A&AS*, 100, 647
- Chiappini, C., Matteucci, F., Gratton, R., 1997, *ApJ*, 477, 765
- Edvarsson, B., Andersen, J., Gustafsson, B., Lambert, D.L., Nissen, P.E., Tomkin, J., 1993, *A&A*, 275, 101
- Fagotto, F., Bressan, A., Bertelli, G., Chiosi, C., 1994a, *A&AS*, 104, 365
- Fagotto, F., Bressan, A., Bertelli, G., Chiosi, C., 1994b, *A&AS*, 105, 29
- Gallart, C., Aparicio, A., Bertelli, G., Chiosi, C., Vilchez, J.M., 1994, *ApJ*, 425, L9
- Gallart, C., Aparicio, A., Bertelli, G., Chiosi, C., 1996, *AJ*, 112, 1950
- Grenon, M., Mermilliod, M., Mermilliod, J.C., 1992, *A&A*, 258, 88
- Kurucz, R.I., 1992 in *Stellar Populations in Galaxies*, eds. B. Barbuy and A. Renzini, p. 225. Dordrecht: Kluwer
- Perryman, M.A.C., Lindegren, L., Kovalevsky, J., Turon, C., Hog, E., Grenon, M. et al., 1995, *A&A*, 304, 69
- Turon, C. et al., 1992, *The Hipparcos Input Catalogue*, ESA SP-1136, p.24
- Vallenari, A., Chiosi, C., Bertelli, G., Ortolani, S., 1996a, *A&A*, 309, 358
- Vallenari, A., Chiosi, C., Bertelli, G., Aparicio, A., Ortolani, S., 1996b, *A&A*, 309, 367